© 2017. Published by The Company of Biologists Ltd | Development (2017) 144, 1296-1306 doi:10.1242/dev.141085

RESEARCH ARTICLE

CDX2 is essential for cell proliferation and polarity in porcine blastocysts

Gerelchimeg Bou[1,2], Shichao Liu[1], Mingju Sun[1], Jiang Zhu[1], Binghua Xue[1], Jia Guo[1], Yueming Zhao[1], Bo Qu[3], Xiaogang Weng[1], Yanchang Wei[1], Lei Lei[4] and Zhonghua Liu[1,5,*]

ABSTRACT

The role of CDX2 in trophectoderm (TE) cells has been extensively studied, yet the results are contradictory and species specific. Here, CDX2 expression and function were explored in early porcine embryos. Notably, siRNA-mediated gene knockdown and lentivirus-mediated TE-specific gene regulation demonstrated that CDX2 is essential for the maintenance of blastocyst integrity by regulating the BMP4-mediated blastocyst niche and classic protein kinase C (PKC)-mediated TE polarity in mammalian embryos. Mechanistically, *CDX2*-depleted porcine embryos stalled at the blastocyst stage and exhibited apoptosis and inactive cell proliferation, possibly resulting from BMP4 downregulation. Moreover, TE cells in *CDX2*-depleted blastocysts displayed defective F-actin apical organization associated with downregulation of PKCα (*PRKCA*). Collectively, these results provide further insight into the functional diversity of CDX2 in early mammalian embryos.

KEY WORDS: CDX2, TE polarity, Cell proliferation, BMP4, PKCα

INTRODUCTION

After several cleavage divisions, mammalian zygotes develop into blastocysts comprising two distinct cell groups: the trophectoderm (TE) and inner cell mass (ICM). The TE is a single layer of polarized epithelial cells that forms the outer wall of the blastocyst and eventually develops into the fetal placenta, whereas the ICM comprises pluripotent cells and eventually develops into the embryo proper. As the earliest-born epithelial cells of mammalian embryos, the TE displays tissue characteristics that are typical of adult epithelia, including a concerted action of cell adhesion molecules, intercellular junctions and an extensive system of intermediate filaments that ensure epithelial integrity and polarized cytoplasmic organization (Fleming et al., 1992; Wiley, 1988). In turn, TE integrity is essential for blastocyst expansion, embryonic patterning, nutrition and implantation.

In mice, TE identity is maintained through a gene regulatory network (GRN) that is orchestrated by the transcription factor, caudal-related homeobox protein 2 (CDX2) (Johnson, 2009). CDX2 is first detected in some nuclei of the 8- to 16-cell stage mouse embryo, and its expression later expands to all blastocystic TE cells (Strumpf et al., 2005; Ralston and Rossant, 2008). CDX2 is one of the earliest transcription factors exhibiting differential expression on the outside and inside of blastomeres. Before the blastocyst stage, CDX2 becomes spatially restricted to the outer blastomeres immediately before the downregulation of OCT4 (*POU5F1*), NANOG and SOX2 (Cockburn and Rossant, 2010). Overexpression of *Cdx2* alone is sufficient to commandeer the whole TE GRN and override mouse embryonic stem (ES) cell pluripotency to induce morphologically and functionally normal trophoblast stem cells (Niwa et al., 2005; Strumpf et al., 2005). *Cdx2*$^{-/-}$ mouse embryos lose TE epithelial integrity and die around the time of implantation (Strumpf et al., 2005), and exogenous *Cdx2* titration into early blastomeres changes the number of cells allocated to forming the TE and ICM by altering cell polarity (Jedrusik et al., 2008). Collectively, these data suggest that *Cdx2* expression before blastocyst formation plays a pivotal role in TE identity and function in mice.

However, reports on CDX2 function before blastocyst formation are contradictory. Several studies have shown that CDX2 is not required for development of the mouse cleavage stage or for apical polarization and viability of mouse TE cells (Blij et al., 2012; Ralston and Rossant, 2008; Strumpf et al., 2005; Wu et al., 2010). These studies demonstrate that mouse embryos depleted of *Cdx2* through either gene knockout or RNA interference (RNAi) are able to develop to normal blastocysts in terms of overall cell number, ICM:TE ratio, and TE apical polarity, despite abnormal cell junctions. Furthermore, *Cdx2*-deficient blastomeres allocate a normal number of cells to the TE in chimeric embryos (Ralston and Rossant, 2008). Despite using the same gene knockout and RNAi approaches, these results are directly contradictory to those reported in other studies, which have shown that *Cdx2* depletion compromises cell polarity and induces developmental arrest before the blastocyst stage, as well as significantly reducing blastocyst rate (the ability of zygotes to normally develop into blastocysts) (Jedrusik et al., 2010, 2015). One plausible explanation for this discrepancy could be the different genetic backgrounds among strains. Nevertheless, given the contradictions and ambiguities, the molecular mechanisms associated with CDX2 function in mouse embryos remain elusive.

CDX2 is also expressed during the early embryonic development of other mammals; however, unlike in mouse, CDX2 protein is detectable after blastocyst formation in humans (Niakan and Eggan, 2013) and at the morula stage in monkeys (Sritanaudomchai et al., 2009). In pigs and cows, CDX2 is specifically expressed in blastocyst TE cells (Kuijk et al., 2008). Functional analysis of CDX2 in preimplantation embryos using RNAi has revealed that monkey blastocysts fail to hatch (Sritanaudomchai et al., 2009), similar to the mouse, whereas bovine blastocysts hatched normally (Berg et al., 2011). Taken together, these results indicate that although CDX2 is

[1]College of Life Science, Northeast Agricultural University, Harbin 150030, China. [2]College of Animal Science, Inner Mongolia Agricultural University, Huhhot 010018, China. [3]Life Science and Biotechnique Research Center, Northeast Agricultural University, Harbin 150030, China. [4]Department of Histology and Embryology, Harbin Medical University, Harbin 150081, China. [5]Key Laboratory of Animal Genetics, Breeding and Reproduction, Education Department of Heilongjiang Province, Harbin 150030, China.

*Author for correspondence (liuzhonghua@neau.edu.cn; liu086@yahoo.com)

Z.L., 0000-0002-9199-6493

Received 24 June 2016; Accepted 3 February 2017

Development (2017) 144, 1296-1306 doi:10.1242/dev.141085

important for early embryonic development, it exhibits functional diversity among species. As such, it is necessary to study *CDX2* in multiple species to fully elucidate its function, and these studies will undoubtedly shed light on the molecular regulation of preimplantation development across mammalian species.

In the present study, porcine CDX2 expression was assessed at both mRNA and protein levels in successive stages of preimplantation embryos. In addition, the CDX2 function in porcine embryonic development was systematically explored using siRNA-mediated gene knockdown and lentivirus-mediated TE-specific gene regulation.

RESULTS

CDX2 spatiotemporal expression pattern in early-stage porcine embryos

To date, CDX2 expression has only been shown in porcine blastocysts. To gain better insights into the role of CDX2 in early embryonic development, the spatial and temporal dynamics of CDX2 were assessed in early porcine embryos. CDX2 was detected in a subset of TE nuclei in cavitated day (D)5 blastocysts (∼20 cells), and in all TE cells in expanded D6.5 and hatched D7.5 blastocysts (Fig. 1A). No CDX2 signal was observed in the nuclei of cleavage-stage embryos and the ICM. Interestingly, OCT4 (Fig. 1A) was present in all cells of the embryos, even in D7.5 hatched blastocysts. *In vivo* staining of CDX2 and OCT4 in porcine embryos at these stages was identical to that of *in vitro* counterparts (Fig. S1A,B versus Fig. 1A). Quantitative real-time PCR (qPCR) results indicated that *CDX2* mRNA expression was remarkably increased at the 16-cell stage just before blastocyst formation, but *OCT4* mRNA was steadily expressed during all developmental stages (Fig. 1B). Consistent with the previous RNA sequencing data (Cao et al., 2014), RT-PCR results confirmed the absence of two other CDX family members, *CDX1* and *CDX4* (three technical replicates, Fig. S1C). Moreover, western blot (WB) analysis revealed that meiosis II (MII)-stage oocytes expressed CDX2, but only ∼1/400 of that present in D6.5 blastocysts (Fig. 1C). Fluorescence *in situ* hybridization of RNA (RNA-FISH) was performed to further confirm the *CDX2* mRNA expression in early porcine embryos, which clearly showed a perinuclear localization (Fig. 1D). The high fluorescence intensity of RNA-FISH was also seen at the 16-cell stage, consistent with our qPCR results (Fig. 1B).

CDX2 knockdown affects total cell number and the hatching process in blastocysts without affecting preceding embryonic development

To address CDX2 function in early porcine embryonic development, modified Stealth siRNA against *CDX2* mRNA (siCDX2) (Fig. S1D) was injected into porcine zygotes, which were then cultured *in vitro* for 7 days. Stealth siRNA effectively decreased target gene expression for 3-4 days, during which time mouse embryos develop from zygotes to blastocysts (Wu et al., 2010). Porcine embryos require ∼7 days to develop from zygotes into blastocysts *in vitro*. As such, *CDX2* expression was evaluated by performing qPCR at different developmental stages after injection of siRNA into zygotes to monitor the efficacy of the injected siRNA. Embryos that had been injected with a scrambled siRNA duplex were used as the control group (siControl embryos), and we set *CDX2* expression in siControl embryos as 100%. As expected, *CDX2* expression was effectively downregulated at least 80% in siCDX2 embryos at D7 and earlier (Fig. 2A). The effective *CDX2* knockdown was also verified by performing RNA-FISH at the four-cell and blastocyst stages (Fig. 2B), and by performing immunofluorescent staining of blastocysts (Fig. 2C).

The cleavage rate and D7.5 blastocyst rate were consistent between siCDX2 and siControl embryos; however, the hatching rate was significantly lower in D7.5 siCDX2 blastocysts compared with the siControl group [0% (0/47) with siCDX2 versus 32% (16/50) with siControl] (Fig. 2D; Fig. S1G,H). In addition, the cell number

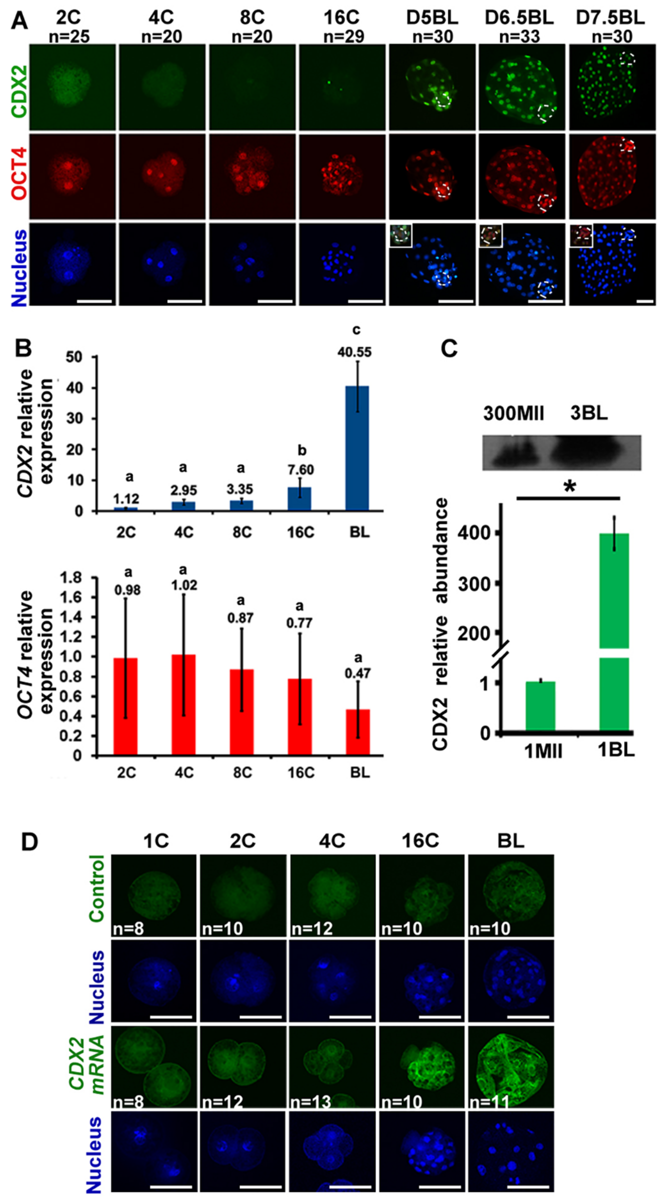

Fig. 1. Spatiotemporal expression pattern of *CDX2* in early-stage porcine embryos. (A) Immunofluorescence images (epifluorescence microscope) for CDX2 and OCT4 expression at different developmental stages. Dashed lines indicate the ICM. *n*, number of tested embryos. Merged images of the ICM region are shown in the corner of the last row of images. 'C' indicates number of cells in the embryo. (B) *CDX2* and *OCT4* mRNA expression levels relative to their MII-stage expression level (set as 1). Data indicate mean±s.d. (six technical replicates). Different characters (a, b, c) above the bars indicate significant differences from each other at $P<0.05$ using one-way ANOVA with Tukey's post-hoc testing. (C) WB analysis for CDX2 protein in 300 MII-stage oocytes (300MII) and three blastocysts (3BL). CDX2 protein abundance per MII-stage oocyte (1MII) and per D6 blastocyst (1BL) are compared in the bar chart. $^*P<0.05$. (D) RNA-FISH for *CDX2* in early-stage porcine embryos. The sense mRNA of *CDX2* was used as a probe in the control group. MII, MII-stage porcine oocytes; BL, blastocyst. *n*, number of tested embryos. Scale bars: 50 µm.

Development (2017) 144, 1296-1306 doi:10.1242/dev.141085

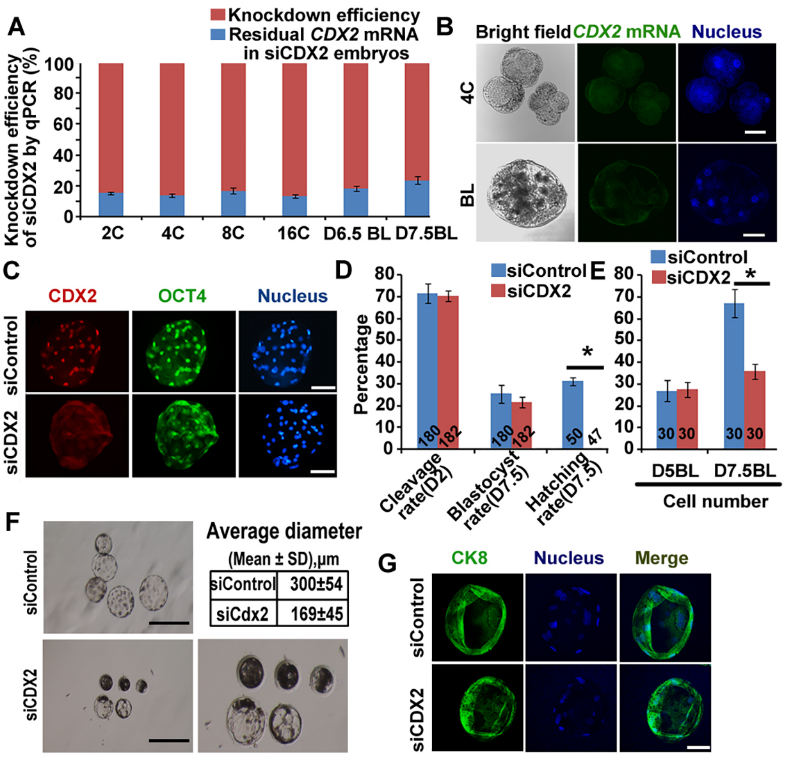

Fig. 2. The effects of *CDX2* knockdown on early porcine embryonic development. (A) qPCR was used to confirm *CDX2* knockdown at all embryonic stages examined. 'C' indicates number of cells in the embryo. (B) RNA-FISH for *CDX2* after siRNA injection. The images of paralleled control groups are shown in Fig. 1D. Scale bars: 50 μm. (C) Immunofluorescence assay comparing CDX2 and OCT4 expression in D6.5 siCDX2 (n=15) and siControl (n=12) blastocysts (BL). Scale bars: 50 μm. (D) Developmental rates of siCDX2 and siControl embryos. Numbers on bars indicate the total number of embryos analyzed. *P<0.05 (Student's t-test). (E) Cell numbers in D5 and 7.5 siCDX2 and siControl blastocysts. Numbers on bars indicate the total number of embryos analyzed. *P<0.05 (Student's t-test). (F) The morphologies and diameters of D7.5 siCDX2 and siControl blastocysts. Scale bars: 500 μm. (G) Sectional confocal images of CK8 in D7.5 siCDX2 (n=15) and siControl (n=15) blastocysts. Scale bar: 50 μm.

was significantly lower in D7.5 siCDX2 blastocysts (Fig. 2E), which were smaller in size compared with the siControl group (Fig. 2F). Cytokeratin 8 (CK8) is a TE-specific intermediate filament and serves as a marker of epithelization. Notably, positive CK8 immunofluorescence signals were observed in the TE of siCDX2 blastocysts, indicative of normal epithelization (Fig. 2G), while the comparable cell numbers between D5 siCDX2 and siControl blastocysts showed that cell proliferation was compromised after blastocyst formation in siCDX2 embryos (Fig. 2E). These results imply that *CDX2* knockdown affects total cell number and the hatching process in blastocysts, independent of previous embryonic development.

CDX2 is dispensable in blastomere polarization and junction formation before the blastocyst stage

Polarization and adherens junctions have appeared by the eight-cell stage in both murine (Eckert and Fleming, 2008; Watson, 1992) and porcine (Reima et al., 1993) embryos, but the role of CDX2 in these events is still under debate. Thus, we investigated *CDX2* function in blastomere polarization given that *CDX2* mRNA expression was observed during cleavage (Fig. 1B; Fig. S1C). F-actin has been widely used as a mouse blastomere polarization marker (Johnson, 2009; Stephenson et al., 2010); therefore, we assessed the effect of *CDX2* knockdown on eight-cell porcine embryo polarization by F-actin staining (Fig. 3A). These results showed that F-actin underwent normal apical polarization at the eight-cell stage in both siCDX2 and siControl embryos. Moreover, staining of E-cadherin (*CDH1*) demonstrated that adherens junction assembly was also intact in eight-cell siCDX2 embryos (Fig. 3B). To confirm these findings, the expression of *CDH1* and other genes associated with polarization (*PAR1* and *PAR3*, *F2R* and *PARD3*, respectively), cell junctions and compaction (*CTNNB1*, encodes β-catenin), and cavitation (*ATP1B1*, encodes a Na^+/K^+-ATPase subunit) were examined by performing qPCR, which showed equivalent levels of expression of these genes in eight-cell siCDX2 and siControl embryos (P>0.05; Fig. 3C). Collectively, these results suggest that CDX2 is not required to establish cell polarity and junctions before blastocyst formation.

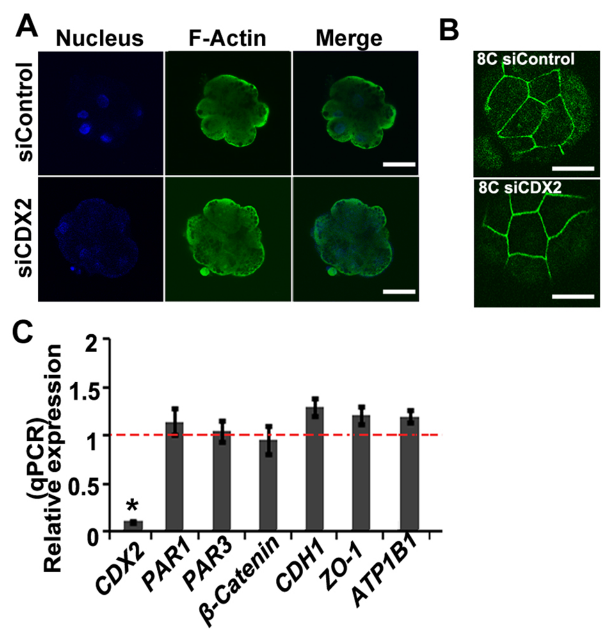

Fig. 3. CDX2 is dispensable for polarization of, and junctions in, cleavage-stage porcine embryos. (A) Sectional confocal images of F-actin in siCDX2 (n=10) and siControl (n=8) eight-cell stage embryos. Scale bars: 50 μm. (B) Sectional confocal images of E-cadherin immunofluorescence staining in siCDX2 (n=12) and siControl (n=10) eight-cell stage embryos. Scale bars: 50 μm. (C) qPCR analysis of *CDX2*, *PAR1*, *PAR3*, *CTNNB1* (β-catenin), *CDH1*, *ZO1* and *ATP1B1* in siCDX2 eight-cell stage embryos. Data indicate $2^{-\Delta\Delta Ct}$ mean±s.d. (three technical replicates). The expression levels in siControl embryos are set as 1 (red line). *P<0.05 compared to the expression level in siControl (Student's t-test).

Development (2017) 144, 1296-1306 doi:10.1242/dev.141085

CDX2 maintains TE cell polarity by regulating PKCα expression

CDX2 depletion did not affect the initial formation of polarity and junctions; however, whether *CDX2* depletion affects later blastocyst stages has not been determined. As such, TE apical polarity was examined by F-actin immunostaining and scanning electron microscopy (SEM). Our results showed that F-actin localized apically on siControl blastocysts, but was more evenly distributed in cytoplasm of siCDX2 blastocysts (Fig. 4A). Given that apical F-actin is crucial to establish microvilli, SEM also showed hindered apical microvilli development on TE cells of siCDX2 embryos as compared to siControl counterparts (Fig. 4B). Due to the important role of F-actin in stress fibers (Tojkander et al., 2012), improper F-actin organization might be a potential reason for the hatching failure of siCDX2 blastocysts. Moreover, SEM images clearly showed that the lack of apical microvilli in siCDX2 blastocysts also influenced formation of the superficial ridge structure between cell-cell contacts, which is generally composed of microvilli from two adjacent epithelial cells (Gorelik et al., 2003). To determine the key factors mediating the deficient TE polarization and apical microvilli formation in siCDX2 blastocysts, qPCR was performed to analyze genes involved in these processes, such as *ACTB*, *EZRIN*, *ARP2*, *CAPZA1* and *PRKCA*. The results showed that *CDX2* depletion did not disturb *ACTB*, *EZRIN*, *ARP2* or *CAPZA1* mRNA expression, whereas *PRKCA* was significantly decreased ($P<0.05$) (Fig. 4C).

PRKCA is an important signal transducer that participates in cytoskeleton organization and function (Hong et al., 2011; Ng et al., 2001). As such, *PRKCA* expression was analyzed using qPCR during early porcine embryo development to determine whether its suppression was responsible for the abnormal apical polarity observed in siCDX2 blastocysts. Interestingly, *PRKCA* was maternally expressed in MII oocytes (Fig. 4D), which might be related to its roles in oocyte meiotic maturation and fertilization (Capo-Chichi et al., 2005; Fan et al., 2002). Thereafter, *PRKCA* expression decreased and remained at a low level until it significantly increased during morula-blastocyst transition (Fig. 4D), which corresponds to the period of CDX2 accumulation in the TE. To evaluate whether *PRKCA* expression is directly regulated by CDX2, we analyzed its expression using qPCR at 36 h after TE-specific lentivirus-mediated *CDX2* overexpression or knockdown in D5 blastocysts (Fig. S2A,B). Notably, *CDX2*-knockdown (CDX-miR) embryos showed significantly lower *PRKCA* expression, whereas those with TE-specific red fluorescent protein-tagged *CDX2* (CDX-RED) showed a marked increase when compared with that in controls that had been infected with lentivirus harboring negative control miRNA (Con-miR) or nucleus-localized red fluorescent protein (NLS-RED), or uninfected intact embryos. After a positive correlation between *CDX2* and *PRKCA* expression was found, the effect of *PRKCA* on TE polarity was examined using siRNA knockdown in porcine embryos. These results demonstrated that *PRKCA* disruption produced the same partial phenotypes as *CDX2* knockdown, including the failure to hatch (Fig. 4F,G), decreased blastocyst cell number ($P<0.05$, Fig. 4H) and loss of TE apical polarity (Fig. 4I).

Previous studies have indicated that phosphorylated EZRIN (p-EZRIN) acts as a bridge between F-actin and plasma membrane proteins during apical polarization, and that PKCα directly phosphorylates EZRIN (Baiocchi et al., 2008; Hong et al., 2011; Ng et al., 2001; Ren et al., 2009). Thus, EZRIN, p-EZRIN, CDX2 and PKCα levels were analyzed by western blotting of blastocysts that had been injected with siCDX2 or an siRNA against *PRKCA* (siPKCα). As expected, p-EZRIN was significantly lower in siCDX2 and siPKCα blastocysts when compared with that in siControl blastocysts (Fig. 4J); however, total EZRIN protein levels did not change. Moreover, *CDX2* depletion reduced PKCα expression, but PKCα depletion did not affect CDX2 levels (Fig. 4J), indicating that PKCα is downstream of CDX2. These results were confirmed by immunostaining of p-EZRIN, which showed that both siCDX2 and siPKCα blastocysts lacked apically localized p-EZRIN (Fig. 4K). Collectively, these results strongly suggest that CDX2 is essential for maintaining cell polarity in the TE through induction of PKCα expression.

Since epithelial cell junctions and apical polarity are mutually dependent (Shin et al., 2006; Tepass, 2012), TE cell junctions were examined in siCDX2 blastocysts. Tight junctions are formed as a rather late molecular event that relies on both cell polarization and intact adherens junctions (Eckert and Fleming, 2008; Sheth et al., 2006). Immunostaining of ZO-1 (*TJP1*) at different developmental stages confirmed that tight junctions were established at the morula stage in porcine embryos (Fig. S3A). Moreover, we found that ZO-1 mRNA expression (Fig. 4L) and protein assembly was normal in siCDX2 embryos at D6.5 (Fig. S3B), but the mRNA was significantly upregulated at D7.5 (Fig. 4L, $P<0.05$). Additionally, although *CDH1* mRNA levels were comparable in siCDX2 and siControl embryos (Fig. 4L), E-cadherin localization was more diffuse at the TE cell border in siCDX2 blastocysts (Fig. 4M), implying that adherens junctions in porcine TE are disrupted in the absence of *CDX2* expression. Therefore, disrupted lateral junction formation, which is important for cavity sealing, could be another factor that aggravates the hatching failure of siCDX2 blastocysts, and this has been observed in mice (Strumpf et al., 2005; Wu et al., 2010).

CDX2 is important to blastocyst cell viability and proliferation, possibly by maintaining the BMP4 mediated blastocyst niche

To gain further insight into the decreased cell number in *CDX2*-deficient blastocysts, apoptosis was assessed via cleaved caspase 3 (Fig. 5A) and terminal deoxynucleotidyl transferase dUTP nick end labeling (TUNEL) staining (Fig. 5B). Consistent with our observations, quantification of TUNEL analysis indicated a high-rate of apoptosis in siCDX2 blastocysts (Fig. 5C).

Subsequently, we examined the expression of select genes that are related to blastocyst development to evaluate the further development of siCDX2 embryos (Fig. 5D,E). The results showed that genes responsible for TE development – *EOMES*, *ELF5* and *GCM1* – were downregulated in D6.5 siCDX2 blastocysts; *CDH3* (placental cadherin) and *HAND1* (a gene important to placental development) were downregulated in D7.5 siCDX2 blastocysts; and *FGFR2* (a signaling receptor important for elongation) was downregulated in both D6.5 and D7.5 siCDX2 blastocysts (Fig. 5D). However, key transcription factors for ICM development, *SOX2* and *NANOG*, were both significantly upregulated in siCDX2 blastocysts, although mRNA encoding OCT4 was not (Fig. 5E). Immunofluorescence staining indicated that SOX2 expression was retained in the TE of siCDX2 blastocysts, whereas it was repressed in that of siControl blastocysts (Fig. 5F). Moreover, qPCR analysis of genes related to paracrine pro-proliferative factors (Fig. 5G) showed that *BMP4* expression was slightly upregulated ($P>0.05$) in D6.5 siCDX2 blastocysts when compared to that in siControl embryos but that *BMP4* levels subsequently diminished ($P<0.05$) at D7.5 only in siCDX2 blastocysts. The expression of both *LIF* and its receptor *LIFR* were also substantially increased in D7.5 siCDX2

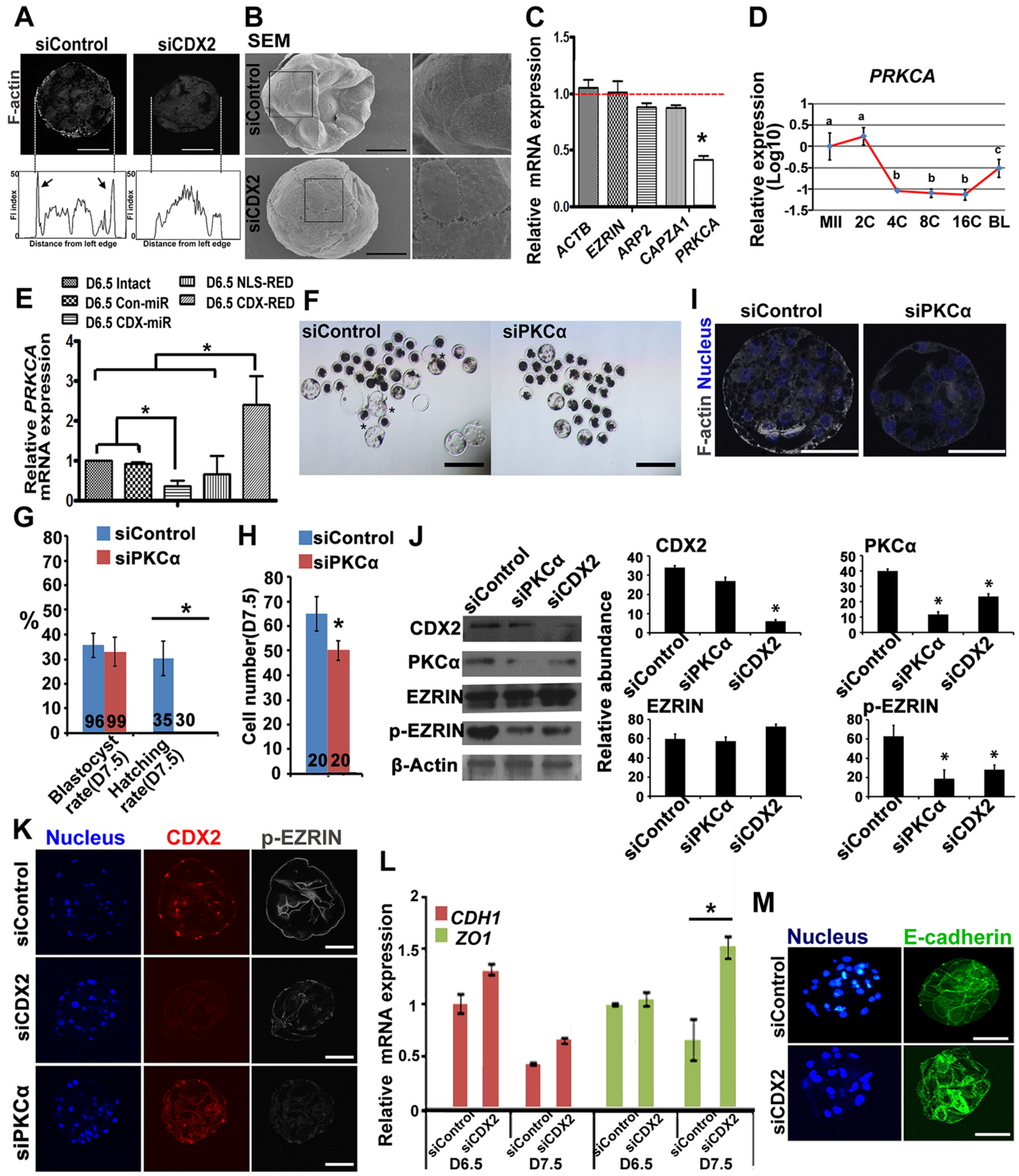

Fig. 4. CDX2 is essential for maintaining the polarity of TE cells via regulation of PKCα expression. (A) Immunostaining of F-actin in D6.5 siCDX2 (*n*=12) and siControl (*n*=13) blastocysts. TE cells in siCDX2 blastocysts lack apical F-actin. Below the immunofluorescence images, the corresponding fluorescence intensities (FI) from the left middle point to the right middle point are plotted (ImageJ software). The arrows on plots indicate the apical polarization of F-actin in siControl blastocysts. (B) The status of superficial microvilli of D6.5 siCDX2 and siControl blastocysts was examined by SEM. Enlarged images are shown on the right. (C) qPCR analysis of genes related to microvilli formation in siCDX2 blastocysts. The values indicate $2^{-\Delta\Delta Ct}$ mean±s.d. (three technical replicates). Gene expression in siControl embryos was set as 1 (red line).**P*<0.05 compared to the expression level in siControl (Student's *t*-test). (D) qPCR analysis of *PRCKA* in preimplantation porcine embryos. Different characters (a, b, c) at data points indicate significant difference from each other (*P*<0.05; one-way ANOVA with Tukey's post-hoc test). (E) qPCR analysis of *PRKCA* expression in D6.5 porcine embryos in which TE-specific alterations of CDX2 had been performed. Intact, uninfected control; Con-miR, infected with virus expressing negative control miRNA; CDX-miR, infected with virus expressing *CDX2* miRNA; NLS-RED, infected with virus expressing nonfunctional nucleus-localizing fluorescent protein; CDX-RED, infected with virus expressing fluorescent protein-tagged CDX2. **P*<0.05 (one-way ANOVA with Tukey's post-hoc test). (F) Hatching failure of siPKCα embryos. * designates hatched control blastocysts. Scale bars: 500 µm. (G) Developmental rate of siPKCα and siControl embryos. (H) Cell numbers in D7.5 siPKCα and siControl blastocysts. In G,H, the numbers shown on the bars indicate the total numbers of embryos analyzed. **P*<0.05 (Student's *t*-test). (I) Sectional confocal images indicated the loss of polarized F-actin in siPKCα embryos. Scale bars: 50 µm. (J) WB images (left) and gray intensity-based quantification (right) of the CDX2, PKCα, EZRIN and phosphorylated EZRIN (p-EZRIN) protein levels in siCDX2, siPKCα and siControl blastocysts. The protein extracts of 100 embryos were loaded per lane. (K) Sectional confocal images showed that p-EZRIN was downregulated in D6.5 siCDX2 and siPKCα blastocysts. Scale bars: 50 µm. (L) qPCR analysis of *CDH1* and *ZO1* expression in siCDX2 blastocysts relative to their expression in D6.5 siControl embryos. The values indicate $2^{-\Delta\Delta Ct}$ mean±s.d. (three technical replicates). **P*<0.05 (Student's *t*-test). (M) Immunofluorescent staining of E-cadherin shows a dispersed distribution in siCDX2 D6.5 blastocysts (*n*=8) compared with that in the siControl D6.5 blastocysts (*n*=10). BL, blastocyst; 'C', number of cells in embryo; MII, MII stage. Scale bars: 50 µm.

blastocysts, while *bFGF* (*FGF2*) expression was comparable between siCDX2 and siControl embryos. However, expression of *FGF4* was decreased, while that of its receptor, *FGFR1*, was increased in D6.5 siCDX2 blastocysts. In mouse blastocysts, CDX2 transcriptionally promotes *Bmp4* expression in TE cells, which is subsequently secreted and binds to the ICM to promote proliferation

Development (2017) 144, 1296-1306 doi:10.1242/dev.141085

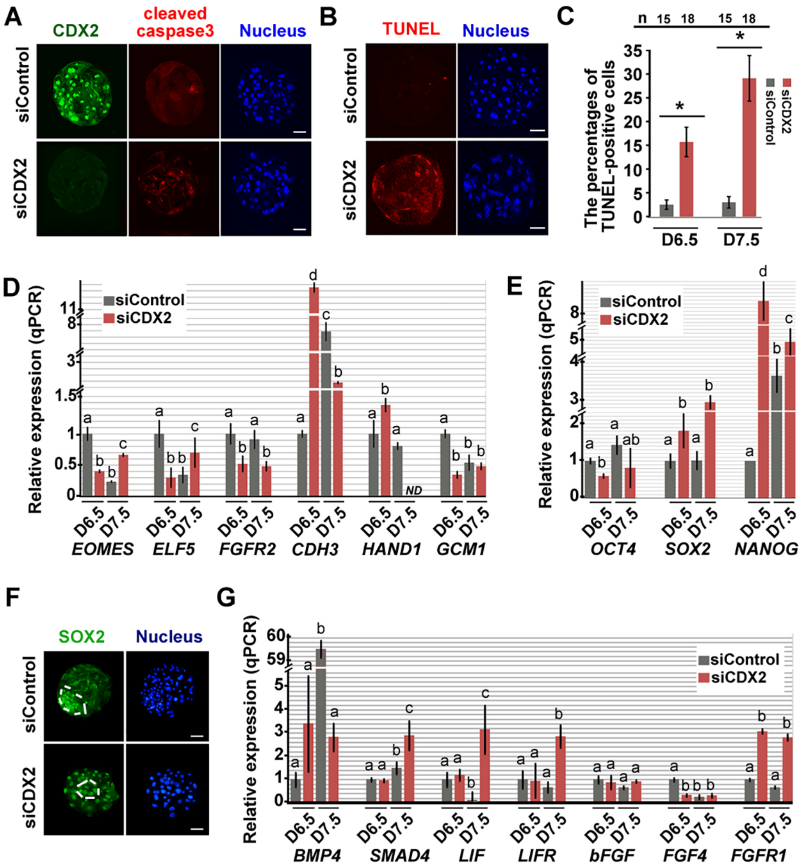

Fig. 5. *CDX2* knockdown increases apoptosis and disturbs gene expression in blastocysts. (A) Comparison of the confocal section images of cleaved caspase3 staining in D6.5 siCDX2 and siControl blastocysts. (B) TUNEL staining of D6.5 siCDX2 and siControl blastocysts. (C) The percentage of TUNEL-positive cells in D6.5 blastocysts. *n*, number of embryos assayed. **P*<0.05 (Student's *t*-test). (D) qPCR analysis of TE-related genes. (E) qPCR analysis of ICM-related genes. (F) *z*-stack confocal images of SOX2 staining of D6.5 siCDX2 and siControl blastocysts. Dashed line indicates the ICM area. Scale bars: 50 μm. (G) qPCR analysis of signaling pathway-related genes. In D, E and G, values are compared with the expression level in D6.5 siControl embryos and indicated as $2^{-\Delta\Delta Ct}$ mean±s.d. (three technical replicates), and the different characters (a, b, c) above the bars indicate significant difference from each other at *P*<0.05, using one-way ANOVA with Tukey's post-hoc testing.

and *Fgf4* expression (Murohashi et al., 2010). In the current study, *BMP4* expression was increased at the blastocyst stage during normal porcine development, consistent with *CDX2* upregulation (Fig. S4B); however, both *BMP4* and *FGF4* were downregulated in siCDX2 blastocysts. In addition, we found that the BMP4 receptor, BMPR2, was expressed specifically in the porcine ICM (Fig. 6A). Together with previous reports of FGF4 expression occurring specifically in the porcine ICM (Fujii et al., 2013), we speculated that the CDX2-BMP4-FGF4 circuit observed in mice (Murohashi et al., 2010) might also be present in porcine embryos.

Based on this rationale, the effect of CDX2-BMP4 regulation on cell proliferation was examined in blastocysts that had been infected

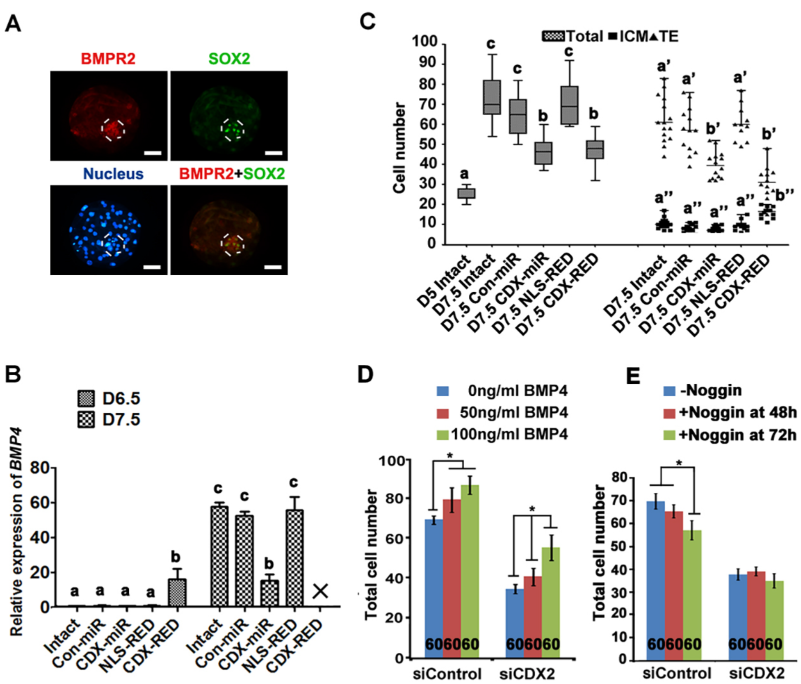

Fig. 6. CDX2 is crucial for blastocyst cell viability and proliferation through BMP4 signaling. (A) The epifluorescence images show that BMPR2 is mainly expressed in the ICM cells (SOX2-positive) of porcine blastocysts. The dashed line in the images indicate the ICM. Scale bars: 50 μm. (B) qPCR analysis of *BMP4* expression after lentivirus-mediated TE-specific *CDX2* regulation. All values are compared with the expression in D6.5 intact embryos and are given as $2^{-\Delta\Delta Ct}$ mean±s.d. (three technical replicates). Different characters (a, b, c) above the bars indicate significant difference from each other at *P*<0.05 using one-way ANOVA with Tukey's post-hoc testing. The cross on the last bar indicates the embryonic degeneration of D7.5 CDX-RED embryos. (C) Box plot of total, ICM and TE cell numbers after TE-specific *CDX2* regulation with the indicated constructs (see Fig. 4) . Different characters a, b, c (total); a′, b′, c′ (TE); or a", b", c" (ICM) above the bars/plots indicate significant within-groups differences from each other at *P*<0.05 using the one-way ANOVA with Kruskal–Wallis test with Dunn's correction. Lines represent medians, boxes represent interquartile ranges, whiskers represent 1.5 times the interquartile range. (D) Blastocyst cell numbers after treatment with different concentrations of BMP4. (E) Blastocyst cell numbers after 48 or 72 h of treatment with BMP4 antagonist Noggin. In D and E, the numbers shown on bars indicates the total number of embryos tested; **P*<0.05 (using the one-way ANOVA with Kruskal–Wallis test and Dunn's correction.).

Development (2017) 144, 1296-1306 doi:10.1242/dev.141085

with TE-specific CDX-miR- or CDX-RED-encoding lentivirus. Notably, *BMP4* expression was significantly higher in *CDX2*-overexpressing blastocysts at D6.5 than that in knockdown or control embryos (Fig. 6B). However, *CDX2*-overexpressing blastocysts severely degenerated at D7.5, most likely resulting from a harmful CDX2 overdose (Bou et al., 2016) (Fig. S2B). In TE-specific *CDX2*-knockdown embryos, *BMP4* failed to increase at D7.5 and was significantly lower than that observed in the three control groups (Fig. 6B). Meanwhile, the mean number of ICM cells in D7.5 blastocysts was significantly increased ($P<0.05$) after TE-specific *CDX2* overexpression, although the mean total of cells in the blastocyst and number of TE cells were decreased, most likely because of TE degeneration (Fig. 6C). Furthermore, both the blastocyst total cell number and TE cell number were significantly reduced in TE-specific *CDX2*-knockdown embryos compared to those in the three control groups (Fig. 6C).

To confirm the functional significance of BMP4 on porcine blastocyst proliferation, cell numbers were determined in D7.5 blastocysts that had been treated with BMP4 or the BMP4 antagonist Noggin, starting on D5. As expected, BMP4 addition significantly increased cell number in both siControl and siCDX2 blastocysts (Fig. 6D; Fig. S4A), whereas Noggin application inhibited cell proliferation specifically in siControl blastocysts (Fig. 6E), indicating that *BMP4* is essential for porcine blastocyst proliferation.

Collectively, these results support our conjecture and suggest that CDX2 is important to blastocyst cell viability and proliferation, possibly by maintaining the BMP4-mediated blastocyst niche in pigs.

CDX2-overexpressing blastomeres preferentially contribute to TE development

Mouse studies have shown that CDX2 is heterogeneously expressed in early blastomeres at the cleavage stage (Dietrich and Hiiragi, 2007), which is believed to contribute to lineage specification (Niwa et al., 2005). However, data from several studies show contradictory effects following the regulation of *Cdx2* levels in early blastomeres (Jedrusik et al., 2008; Ralston and Rossant, 2008). Thus, we examined whether regulating *CDX2* levels in porcine blastomeres during cleavage influences their developmental fate. For this, siCDX2 or *CDX2* mRNA, along with an episomal plasmid expressing EGFP (pS/MAR-EGFP), were injected into one blastomere of a four-cell porcine embryo, and the distribution of EGFP-positive cells was traced in blastocysts (Fig. 7A). Results showed that the blastocysts segregated into three groups: ‘ICM only’ (all EGFP-positive cells contributed to the ICM), ‘TE only’ (all EGFP-positive cells contributed to the TE) or ‘ICM&TE’ (positive cells were found in both the ICM and TE) (Fig. 7B). Interestingly, the proportion of TE-only embryos was significantly increased in the *CDX2*-overexpressing group (Fig. 7C; $P<0.05$), whereas no significant difference was found between the *CDX2*-knockdown and control groups. Thus, these data suggest that CDX2 plays an important role in the GRN controlling the molecular features of the TE in porcine embryos but that CDX2 is insufficient to determine TE fate.

DISCUSSION

Genes are known to show species-specific expression patterns or functions in mammals. For example, *Cdx2* expression in early mouse embryos resembles neither that in humans (Niakan and Eggan, 2013) nor monkeys (Sritanaudomchai et al., 2009). CDX2 is a major regulator of initial lineage segregation and trophoblast stem cell properties. The current study indicates that the CDX2 expression pattern in porcine embryos is relatively similar to that of humans, in which CDX2 is upregulated in TE cells after blastocyst formation (Niakan and Eggan, 2013). As such, exploring CDX2 function in porcine embryos might enhance our knowledge of molecular regulation in embryology in general and shed light on the function of CDX2 during human development.

The spatiotemporal expression of CDX2 in porcine embryo differs from that of mouse embryo (Dietrich and Hiiragi, 2007) (Fig. 7D). In mice, CDX2 protein is first detected in some blastomeres of eight-cell stage embryos and its expression becomes restricted to the TE by E3.5. In contrast, porcine CDX2 protein is initially observed in some TE cells right after cavitation at E5 and remains exclusively in the TE thereafter. Interestingly, the time point for porcine CDX2 protein expression is very similar to that in bovine (Goissis and Cibelli, 2014; Madeja et al., 2013) and human (Niakan and Eggan, 2013) embryos, in which CDX2 protein becomes detectable after blastocyst formation. Similarly, prolonged OCT4 expression in the TE is also observed in human (Cauffman et al., 2005) and bovine (van Eijk et al., 1999) embryos. Since CDX2 accumulation is primed by Hippo signaling in response to cell contact and positional information in mice (Hirate and Sasaki, 2014; Nishioka et al., 2009), it would be interesting to explore whether this signaling pathway exists in porcine embryos, as this knowledge would expand our mechanistic understanding of the various *CDX2* expression patterns observed in mammalian embryos.

The current data on CDX2 function in mouse embryos before blastocyst formation is contradictory (Bruce, 2011; Wu and Schöler, 2011). Our results, derived from *CDX2*-knockdown porcine embryos, indicate that CDX2 is not essential before blastocyst formation, since the siCDX2 blastocyst rate was no different from that of the control. This result is consistent with several studies in mice, which show that *Cdx2*-mutant (Strumpf et al., 2005) or knockdown (Wu et al., 2010) embryos develop normally to the blastocyst stage; however, others have found that *Cdx2* depletion induces developmental arrest before blastocyst formation (Jedrusik et al., 2010, 2015). Different time points for CDX2 accumulation in mice and other mammals might account for the different phenotypes of CDX2-depleted mouse and pig embryos. Therefore, the results from porcine studies may be more pertinent to our understanding of CDX2 function in embryonic development in large animals, including cows and primates, which also show the same temporal pattern of CDX2 accumulation (Goissis and Cibelli, 2014; Madeja et al., 2013; Niakan and Eggan, 2013). However, more studies in various strains are needed to clarify the functional significance of CDX2 in mouse cleavage-stage embryos (Wu and Schöler, 2011).

The effect of CDX2 on mouse TE-fate commitment is still a matter of debate. Results from a study by Jedrusik et al. (2008) indicate that CDX2 is a key factor in TE-fate commitment, as increased *Cdx2* expression in individual blastomeres promotes differentiation towards the TE lineage and hinders that of the ICM. In contrast, Ralston and Rossant (2008) indicate that CDX2 functions downstream of lineage allocation since *Cdx2*-depleted blastomeres do not preferentially contribute to the ICM. Our study found that cell polarization and junctions in siCDX2 porcine embryos before the blastocyst stage were similar to those of controls. Although *CDX2*-overexpressing blastomeres from four-cell stage embryos contributed to the TE at a higher frequency; blastomeres in which *CDX2* had been downregulated did not contribute to the ICM in the same way. Consistent with our results, a bovine study (Goissis and Cibelli, 2014) has indicated that *CDX2*

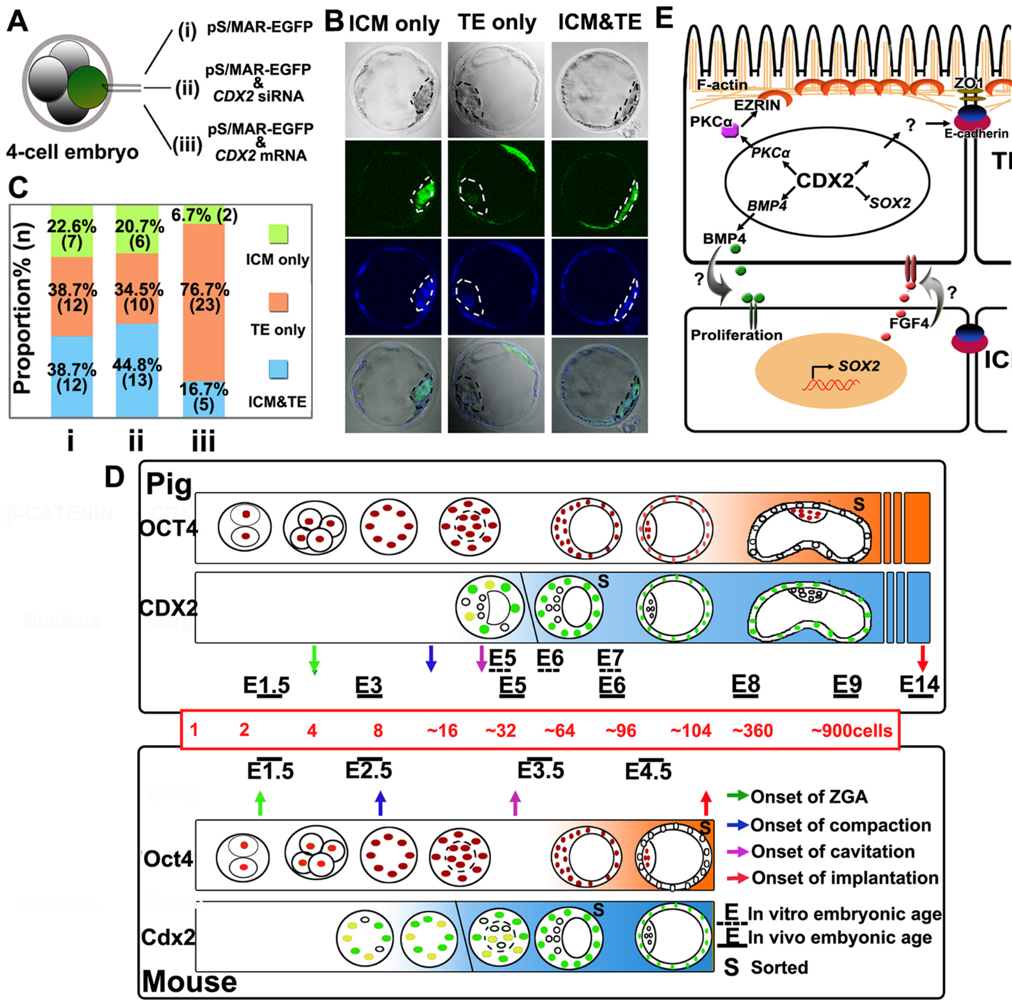

Fig. 7. *CDX2* upregulation in early blastomeres causes a differentiation bias towards the TE lineage. (A) Scheme for the experimental strategy. (B) Representative confocal section images illustrate the three groups of blastocysts. Green, EGFP; blue, DAPI. (C) The proportions of the three types of blastocyst in the three experimental groups shown in A. The percentage and embryo numbers (in brackets) of every type are indicated on the bars. (D) The CDX2 and OCT4 expression patterns in early porcine and mouse embryos [modified based on the mouse pattern in previous literature (Dietrich and Hiiragi, 2007)]. Green and dark red represent strong expression, yellow and light red represent weak expression, and empty circles indicate an absence of nuclear CDX2 or OCT4. (E) Schematic summary of CDX2 functions in porcine blastocysts.

depletion does not affect the blastocyst rate and TE, ICM or total cell number. Interestingly, although CDX2 is first detectable at the morula-stage in monkey embryos, CDX2 knockdown did not affect blastocyst formation (Sritanaudomchai et al., 2009). Collectively, these results suggest that CDX2 is not involved in TE-fate decisions in large animal embryos.

Data regarding the role of CDX2 on TE cells and further development of blastocysts are similar among different studies and different species. In mice, both *Cdx2*-knockout and -knockdown blastocysts exhibit a hatching failure, decreased cell number, abnormal TE cell junctions/polarity and a disturbed TE GRN (Blij et al., 2012; Jedrusik et al., 2010, 2015; Nishioka et al., 2008; Ralston and Rossant, 2008; Strumpf et al., 2005; Wu et al., 2010). In primates (Sritanaudomchai et al., 2009) and cattle (Goissis and Cibelli, 2014; Madeja et al., 2013), *CDX2* knockdown results in a hatching failure and deficient cell proliferation in blastocysts. Consistently, our study also showed that *CDX2* knockdown compromises TE cell polarization and junctions. Furthermore, our results indicate that PKCα is a key intermediary for the effect of CDX2 on TE cell polarity.

A CDX2-BMP4-FGF4 functional circuit has been shown in mouse embryos (Murohashi et al., 2010). Similarly, our study determined that BMP4 promotes blastocyst cell proliferation and is regulated by CDX2 in the TE of porcine blastocysts. This suggests that downregulation of BMP4 in siCDX2 porcine embryos is partially responsible for the deceased cell number, along with the increasing rate of apoptosis. Thus, it is also reasonable to conclude that the hatching-failure phenotype seen in siCDX2 porcine embryos could result from defects in cell proliferation, as well as in TE cell junction/ polarity. Despite the discrepancy between species in CDX2 function before blastocyst formation, CDX2 participation in TE maintenance is clearly necessary for blastocyst development among various mammals.

It is noteworthy that CDX2 plays species-specific roles in regulating trophoblast-related gene expression. Reports from mouse trophoblast stem cell studies show that CDX2, EOMES and ELF5 form a positive-feedback loop that maintains lineage fate (Ng et al., 2008). However, according to a previous study (Valdez Magaña et al., 2014), this loop might not exist in the porcine trophoblast lineage since EOMES and ELF5 are only highly expressed in

Development (2017) 144, 1296-1306 doi:10.1242/dev.141085

tubular-stage porcine embryos, when *CDX2* expression in TE cells has already been downregulated, and ELF5 is not co-expressed with CDX2 in the porcine TE. Thus, it is assumed that CDX2 does not transcriptionally upregulate *EOMES* and/or *ELF5* expression in porcine TE, and it is more likely that CDX2 and EOMES and/or ELF5 control the TE GRN at the early and late stages, respectively. Therefore, higher *EOMES* and *ELF5* levels in siCdx2 D7.5 porcine embryos might occur due to a compensative mechanism following *CDX2* downregulation.

Along with CDX2 studies in other mammalian embryos, the current study of porcine embryos highlights the importance of CDX2 in early mammalian development. In Fig. 7D, we compare preimplantation embryonic development between mouse and pig, *in vitro* and *in vivo*, and include key developmental events such as zygotic genome activation (ZGA), compaction, cavitation and implantation. In addition, the key results of this study are summarized in Fig. 7E. Comparisons of embryonic development among multiple mammalian species will not only improve overall knowledge of mammalian embryonic development but also provide clues to find more suitable animal models for human embryonic development. Collectively, our findings provide new ideas on CDX2 function in human embryonic development, especially with regard to TE development, due to the similarities in CDX2 spatiotemporal expression patterns between pig and human embryos.

MATERIALS AND METHODS

In vitro embryo production and culture

All animal procedures conformed to the guidelines and regulatory standards of the Animal Care and Use Committee of Northeast Agricultural University. Porcine oocytes were matured *in vitro*, as previously described (Liu et al., 2008). To generate *in vitro* fertilization embryos, denuded oocytes were washed and held in modified Tris-buffered medium before fertilization using standard procedures (Abeydeera and Day, 1997). Presumptive zygotes were then cultured in PZM-3 medium (Yoshioka et al., 2002) for 7 days at 39°C under a 5% CO_2 atmosphere. Cleavage rates were evaluated at day 2 using microscopy, whereas blastocyst and hatching rates were assessed at day 7.5. Cell numbers at days 5, 6.5 and 7.5 were quantified by DAPI nuclear staining.

In vivo embryo collection

In vivo embryos were collected from Yorkshire-Danish Landrace sows from days 1 to 6 post insemination. The sows were mated twice within 24 h after detection of estrus, at an interval of 12 h. The last mating time was taken to be day 0 (D0) of conception. Reproductive organs collected from the sows were transported to the laboratory in warm saline (37°C) for a maximum period of 1 h. Embryos were rinsed twice using 50 ml of PBS supplemented with 5% fetal bovine serum (FBS). All procedures were approved by the Animal Ethics Committee of the Northeast Agriculture University, Harbin, China.

Whole-embryo and single-blastomere *CDX2* regulation via RNA injection

Stealth siRNA against porcine *CDX2* designed with BLOCK-iT RNAi Designer was injected into zygotes or one blastomere of a four-cell stage porcine embryo. The most effective duplex (sequence given here) was selected from three Stealth siRNAs: *siCDX2*sense: 5′-CGAAAGACAAA-UACCGAGUCGUGUA-3′; *siCDX2* antisense: 5′-UACACGACUCGGU-AUUUGUCUUUCG-3′.

CDX2 siRNA efficiency and specificity was demonstrated in porcine intestinal epithelial cells (Fig. S1E). At the same time, a scrambled siRNA duplex with the same nucleotide composition but no specific target was used as the control. The sequence of the control siRNA was as follows: siControl sense: 5′-CGAACAGAUAAAGCCGCUGUAAGUA-3′; siControl antisense: 5′-UACUUACAGCGGCUUUAUCUGUUCG-3′.

CDX2 was overexpressed in one blastomere of a four-cell stage porcine embryo through mRNA injection. The *CDX2* full-length open reading frame was cloned from cDNA of a porcine blastocyst and inserted into pMACS KkHA(N) plasmid (Miltenyi Biotec) and used for *in vitro* transcription (RIBOMAX Large Scale RNA Production System T7 kit, Promega). The PCR primers used were as follows: CDX2F: 5′-ATGTACGTGAGCTAC-CTCCTGGACAAGGAC-3′; CDX2R: 5′-CTGGGTGACGGTGGGGTT-TAACACGC-3′.

Microinjection of siRNA or mRNA was performed using an Eppendorf FemtoJet microinjector and Narishige NT-88NE micromanipulators. A glass capillary femtotipII (Eppendorf) was loaded with 5 µl of RNA (20 nM siRNA, 50 ng/µl mRNA) using a microloader (Eppendorf), and about 30 pl of solution was injected into the zygote or blastomere cytoplasm. To trace the fate of the single blastomeres that had been injected, 20 ng/µl of episomal plasmid pS/MAR-EGFP was co-injected with the siRNA or mRNA, or alone as control. Microinjection efficiency in this study was near 100%, as proven by injecting *GFP* mRNA under the same conditions (Fig. S1F).

TE-specific *CDX2* regulation via lentivirus infection of D5 blastocysts

To achieve TE-specific *CDX2* regulation, the zona pellucida was removed from D5 early cavitated embryos with pronase and then washed. Each of 15 blastocysts was then infected in 30 µl of equilibrated PZM3 containing 5×10^6 cfu of lentivirus in mineral oil and incubated at 39°C under 5% CO_2 for 3 h. Infected embryos were then washed and cultured in 500 µl of fresh PZM3. The total numbers of ICM and TE cells were calculated based on intranuclear – CDX2 and OCT4 – and fluorescent signals (Fig. S2C). The procedures for obtaining different lentiviruses with a FUW backbone were described previously (Zhi et al., 2014).

siRNA-mediated knockdown of ZO-1 and PKCα

Stealth siRNAs against porcine *PRKCA* and mRNA encoding ZO-1 were designed using BLOCK-iT RNAi Designer. Because PKCα functions before the first cleavage (Capo-Chichi et al., 2005; Fan et al., 2002), *PRKCA* knockdown was accomplished by injecting siRNA into all blastomeres of two-cell embryos. siRNA against ZO-1 was injected into zygotes for knockdown. Stealth siRNA against mRNAs encoding PKCα and ZO-1 were: siPRKCA sense: 5′-UGGUUCACAAGAGGUGCCAUGAGUU-3′; siPRKCA antisense: 5′-AACUCAUGGCACCUCUUGUGAACCA-3′; and siZO1 sense: 5′-GCGCUACAAGUGAUGACCUUGAUUU-3′; siZO1 antisense: 5′-AAAUCAAGGUCAUCACUUGUAGCGC-3′.

Negative control siRNA (Cat#12935300, Invitrogen) was used as control siRNA for the above knockdown experiments.

RNA-FISH

Embryos were fixed with 4% PFA overnight at 4°C, and stored in methanol at −20°C. *In situ* hybridization was performed as previously described (Chazaud et al., 2006) with slight modifications. RNA probes for porcine *CDX2* were generated by *in vitro* transcription of 936-bp full-length cDNA cloned into the pSPT18 plasmid. The sense and antisense probes were synthesized *in vitro* under control of the T7 and SP2 promoters, respectively, and labeled with digoxigenin-UTP using a DIG RNA labeling kit (SP6/T7) (Roche). The slide was sealed with ProLong Gold antifade reagent (Invitrogen) and visualized on a Leica TCS SP2 confocal microscope with a 40× oil immersion objective.

RNA isolation, cDNA synthesis and qPCR analysis

For real-time analysis of gene expression, 100 oocytes and embryos were harvested in 10 µl RLT buffer and RNA was extracted with PureLink Micro-to-Midi total RNA purification kit with DNAse I treatment (Invitrogen). The cDNA synthesis was performed using High Capacity cDNA reverse transcription kits (ABI).

The cDNA (~8 oocytes/embryos per reaction) was used in 50-µl real-time reactions (SYBR Premix Ex Taq for Perfect Real Time, Takara) using oligonucleotide primers (Table S1). All transcripts levels were normalized against 18S rRNA for oocyte and embryo samples (Kuijk et al., 2007). For porcine intestinal epithelial cells, the 60S ribosomal protein L4 RNA (Nygard et al., 2007) was used as reference gene. qPCR was performed with the ABI 7500 real-time PCR system. Three to six biological and three technical replicates were performed. The $2^{-\Delta\Delta Ct}$ method was used for relative quantification analysis. To determine knockdown efficacy, embryos that had been injected with a scrambled siRNA duplex were used as controls (siControl embryos), and we set *CDX2* expression of siControl embryos as 100%.

WB and immunofluorescence assays

WB and immunofluorescence experiments in porcine embryos were conducted as previously described (Bou et al., 2016) with the antibodies described in Table S2.

Scanning electron microscopy

After removing the zona pellucida, embryos were processed as previously described (Xia et al., 2011) and imaged with a S-3400N (Hitachi) microscope.

TUNEL assay

Apoptosis was determined by using the TUNEL technique. DNA strand breaks were directly labeled with red fluorescence using tetra-methyl-rhodamine-dUTP (*In situ* Cell Death detection kit, TMR red, Roche), as described previously (Hao et al., 2004).

Statistical analysis

Each experiment was repeated at least three times, and representative images are shown in figures. All values are reported as the mean±s.d. Statistical calculations were performed in GraphPad Prism 6 (GraphPad software Inc.). To compare the gene expression levels and embryonic development rate, we used unpaired two-tailed Student's *t*-tests (parametric) or unpaired two-tailed Mann–Whitney *U*-tests (non-parametric) when analyzing two groups. The one-way ANOVA with Tukey's post-hoc testing (parametric) or Kruskal–Wallis test with Dunn's correction for multiple comparisons (non-parametric) was used to analyze multiple groups, mainly when comparing cell numbers. The *F*-test, Browne–Forsythe test or Bartlett's test was used to determine the distributional assumption (normality and homogeneity of variance) of the data. Non-parametric tests were used when data did not fit a normal distribution. Significant differences were defined as $P<0.05$. Differences are shown with *, or different letters a, b, c.

Acknowledgements
We thank Lin Cui and Xuedong Wang (Northeast Agricultural University) for S.E.M. analysis and LetPub (www.letpub.com) for assistance with editing.

Competing interests
The authors declare no competing or financial interests.

Author contributions
G.B. and Z.L. designed the research; G.B., S.L., M.S., J.Z., B.X., J.G. and Y.Z. carried out the research; B.Q. and L.L. contributed reagents/analytical tools; X.W. and Y.W. analyzed data; G.B. and Z.L. wrote the paper.

Funding
This work was supported by the National Basic Research Program of China (Ministry of Science and Technology of the People's Republic of China) [2011CB944202], the National Natural Science Foundation of China [31371457, 31401228] and Fostering Talents in Basic Science of the National Natural Science Foundation of China [J1210069].

Supplementary information
Supplementary information available online at
http://dev.biologists.org/lookup/doi/10.1242/dev.141085.supplemental

References
Abeydeera, L. R. and Day, B. N. (1997). Fertilization and subsequent development in vitro of pig oocytes inseminated in a modified tris-buffered medium with frozen-thawed ejaculated spermatozoa. *Biol. Reprod.* **57**, 729-734.

Baiocchi, L., Tisone, G., Russo, M. A., Longhi, C., Palmieri, G., Volpe, A., Almerighi, C., Telesca, C., Carbone, M., Toti, L. et al. (2008). TUDCA prevents cholestasis and canalicular damage induced by ischemia-reperfusion injury in the rat, modulating PKCalpha-ezrin pathway. *Transpl. Int.* **21**, 792-800.

Berg, D. K., Smith, C. S., Pearton, D. J., Wells, D. N., Broadhurst, R., Donnison, M. and Pfeffer, P. L. (2011). Trophectoderm lineage determination in cattle. *Dev. Cell* **20**, 244-255.

Blij, S., Frum, T., Akyol, A., Fearon, E. and Ralston, A. (2012). Maternal Cdx2 is dispensable for mouse development. *Development* **139**, 3969-3972.

Bou, G., Liu, S., Guo, J., Zhao, Y., Sun, M., Xue, B., Wang, J., Wei, Y., Kong, Q. and Liu, Z. (2016). Cdx2 represses Oct4 function via inducing its proteasome-dependent degradation in early porcine embryos. *Dev. Biol.* **410**, 36-44.

Bruce, A. W. (2011). What is the role of maternally provided Cdx2 mRNA in early mouse embryogenesis? *Reprod. Biomed. Online* **22**, 512-515.

Cao, S., Han, J., Wu, J., Li, Q., Liu, S., Zhang, W., Pei, Y., Ruan, X., Liu, Z., Wang, X. et al. (2014). Specific gene-regulation networks during the pre-implantation development of the pig embryo as revealed by deep sequencing. *BMC Genomics* **15**, 4.

Capo-Chichi, C. D., Rula, M. E., Smedberg, J. L., Vanderveer, L., Parmacek, M. S., Morrisey, E. E., Godwin, A. K. and Xu, X.-X. (2005). Perception of differentiation cues by GATA factors in primitive endoderm lineage determination of mouse embryonic stem cells. *Dev. Biol.* **286**, 574-586.

Cauffman, G., Van de Velde, H., Liebaers, I. and Van Steirteghem, A. (2005). Oct-4 mRNA and protein expression during human preimplantation development. *Mol. Hum. Reprod.* **11**, 173-181.

Chazaud, C., Yamanaka, Y., Pawson, T. and Rossant, J. (2006). Early lineage segregation between epiblast and primitive endoderm in mouse blastocysts through the Grb2-MAPK pathway. *Dev. Cell* **10**, 615-624.

Cockburn, K. and Rossant, J. (2010). Making the blastocyst: lessons from the mouse. *J. Clin. Invest.* **120**, 995-1003.

Dietrich, J.-E. and Hiiragi, T. (2007). Stochastic patterning in the mouse pre-implantation embryo. *Development* **134**, 4219-4231.

Eckert, J. J. and Fleming, T. P. (2008). Tight junction biogenesis during early development. *Biochim. Biophys. Acta* **1778**, 717-728.

Fan, H.-Y., Tong, C., Li, M.-Y., Lian, L., Chen, D.-Y., Schatten, H. and Sun, Q.-Y. (2002). Translocation of the classic protein kinase C isoforms in porcine oocytes: implications of protein kinase C involvement in the regulation of nuclear activity and cortical granule exocytosis. *Exp. Cell Res.* **277**, 183-191.

Fleming, T. P., Javed, Q. and Hay, M. (1992). Epithelial differentiation and intercellular junction formation in the mouse early embryo. *Development* (Suppl.), 105-112.

Fujii, T., Sakurai, N., Osaki, T., Iwagami, G., Hirayama, H., Minamihashi, A., Hashizume, T. and Sawai, K. (2013). Changes in the expression patterns of the genes involved in the segregation and function of inner cell mass and trophectoderm lineages during porcine preimplantation development. *J. Reprod. Dev.* **59**, 151-158.

Goissis, M. D. and Cibelli, J. B. (2014). Functional characterization of CDX2 during bovine preimplantation development in vitro. *Mol. Reprod. Dev.* **81**, 962-970.

Gorelik, J., Shevchuk, A. I., Frolenkov, G. I., Diakonov, I. A., Lab, M. J., Kros, C. J., Richardson, G. P., Vodyanoy, I., Edwards, C. R. W., Klenerman, D. et al. (2003). Dynamic assembly of surface structures in living cells. *Proc. Natl. Acad. Sci. USA* **100**, 5819-5822.

Hao, Y., Lai, L., Mao, J., Im, G. S., Bonk, A. and Prather, R. S. (2004). Apoptosis in parthenogenetic preimplantation porcine embryos. *Biol. Reprod.* **70**, 1644-1649.

Hirate, Y. and Sasaki, H. (2014). The role of angiomotin phosphorylation in the Hippo pathway during preimplantation mouse development. *Tissue Barriers* **2**, e28127.

Hong, S.-H., Osborne, T., Ren, L., Briggs, J., Mazcko, C., Burkett, S. S. and Khanna, C. (2011). Protein kinase C regulates ezrin-radixin-moesin phosphorylation in canine osteosarcoma cells. *Vet. Comp. Oncol.* **9**, 207-218.

Jedrusik, A., Parfitt, D.-E., Guo, G., Skamagki, M., Grabarek, J. B., Johnson, M. H., Robson, P. and Zernicka-Goetz, M. (2008). Role of Cdx2 and cell polarity in cell allocation and specification of trophectoderm and inner cell mass in the mouse embryo. *Genes Dev.* **22**, 2692-2706.

Jedrusik, A., Bruce, A. W., Tan, M. H., Leong, D. E., Skamagki, M., Yao, M. and Zernicka-Goetz, M. (2010). Maternally and zygotically provided Cdx2 have novel and critical roles for early development of the mouse embryo. *Dev. Biol.* **344**, 66-78.

Jedrusik, A., Cox, A., Wicher, K. B., Glover, D. M. and Zernicka-Goetz, M. (2015). Maternal-zygotic knockout reveals a critical role of Cdx2 in the morula to blastocyst transition. *Dev. Biol.* **398**, 147-152.

Johnson, M. H. (2009). From mouse egg to mouse embryo: polarities, axes, and tissues. *Annu. Rev. Cell Dev. Biol.* **25**, 483-512.

Kuijk, E. W., du Puy, L., van Tol, H. T. A., Haagsman, H. P., Colenbrander, B. and Roelen, B. A. J. (2007). Validation of reference genes for quantitative RT-PCR studies in porcine oocytes and preimplantation embryos. *BMC Dev. Biol.* **7**, 58.

Kuijk, E. W., Du Puy, L., Van Tol, H. T. A., Oei, C. H. Y., Haagsman, H. P., Colenbrander, B. and Roelen, B. A. J. (2008). Differences in early lineage segregation between mammals. *Dev. Dyn.* **237**, 918-927.

Liu, Z. H., Song, J., Wang, Z. K., Tian, J. T., Kong, Q. R., Zheng, Z., Yin, Z., Gao, L., Ma, H. K., Sun, S. et al. (2008). Green fluorescent protein (GFP) transgenic pig produced by somatic cell nuclear transfer. *Chin. Sci. Bull.* **53**, 1035-1039.

Madeja, Z. E., Sosnowski, J., Hryniewicz, K., Warzych, E., Pawlak, P., Rozwadowska, N., Plusa, B. and Lechniak, D. (2013). Changes in sub-cellular localisation of trophoblast and inner cell mass specific transcription factors during bovine preimplantation development. *BMC Dev. Biol.* **13**, 32.

Murohashi, M., Nakamura, T., Tanaka, S., Ichise, T., Yoshida, N., Yamamoto, T., Shibuya, M., Schlessinger, J. and Gotoh, N. (2010). An FGF4-FRS2alpha-Cdx2 axis in trophoblast stem cells induces Bmp4 to regulate proper growth of early mouse embryos. *Stem Cells* **28**, 113-121.

Ng, T., Parsons, M., Hughes, W. E., Monypenny, J., Zicha, D., Gautreau, A., Arpin, M., Gschmeissner, S., Verveer, P. J., Bastiaens, P. I. et al. (2001). Ezrin is a downstream effector of trafficking PKC-integrin complexes involved in the control of cell motility. *EMBO J.* **20**, 2723-2741.

Ng, R. K., Dean, W., Dawson, C., Lucifero, D., Madeja, Z., Reik, W. and Hemberger, M. (2008). Epigenetic restriction of embryonic cell lineage fate by methylation of Elf5. *Nat. Cell Biol.* **10**, 1280-1290.

Niakan, K. K. and Eggan, K. (2013). Analysis of human embryos from zygote to blastocyst reveals distinct gene expression patterns relative to the mouse. *Dev. Biol.* **375**, 54-64.

Nishioka, N., Yamamoto, S., Kiyonari, H., Sato, H., Sawada, A., Ota, M., Nakao, K. and Sasaki, H. (2008). Tead4 is required for specification of trophectoderm in pre-implantation mouse embryos. *Mech. Dev.* **125**, 270-283.

Nishioka, N., Inoue, K., Adachi, K., Kiyonari, H., Ota, M., Ralston, A., Yabuta, N., Hirahara, S., Stephenson, R. O., Ogonuki, N. et al. (2009). The Hippo signaling pathway components Lats and Yap pattern Tead4 activity to distinguish mouse trophectoderm from inner cell mass. *Dev. Cell* **16**, 398-410.

Niwa, H., Toyooka, Y., Shimosato, D., Strumpf, D., Takahashi, K., Yagi, R. and Rossant, J. (2005). Interaction between Oct3/4 and Cdx2 determines trophectoderm differentiation. *Cell* **123**, 917-929.

Nygard, A.-B., Jørgensen, C. B., Cirera, S. and Fredholm, M. (2007). Selection of reference genes for gene expression studies in pig tissues using SYBR green qPCR. *BMC Mol. Biol.* **8**, 67.

Ralston, A. and Rossant, J. (2008). Cdx2 acts downstream of cell polarization to cell-autonomously promote trophectoderm fate in the early mouse embryo. *Dev. Biol.* **313**, 614-629.

Reima, I., Lehtonen, E., Virtanen, I. and Fléchon, J. E. (1993). The cytoskeleton and associated proteins during cleavage, compaction and blastocyst differentiation in the pig. *Differentiation* **54**, 35-45.

Ren, L., Hong, S. H., Cassavaugh, J., Osborne, T., Chou, A. J., Kim, S. Y., Gorlick, R., Hewitt, S. M. and Khanna, C. (2009). The actin-cytoskeleton linker protein ezrin is regulated during osteosarcoma metastasis by PKC. *Oncogene* **28**, 792-802.

Sheth, B., Eckert, J., Thomas, F. and Fleming, T. (2006). Tight junctions during development. In *Tight Junctions* (ed. L. Gonzalez-Mariscal), pp. 164-174. USA: Springer.

Shin, K., Fogg, V. C. and Margolis, B. (2006). Tight junctions and cell polarity. *Annu. Rev. Cell Dev. Biol.* **22**, 207-235.

Sritanaudomchai, H., Sparman, M., Tachibana, M., Clepper, L., Woodward, J., Gokhale, S., Wolf, D., Hennebold, J., Hurlbut, W., Grompe, M. et al. (2009). CDX2 in the formation of the trophectoderm lineage in primate embryos. *Dev. Biol.* **335**, 179-187.

Stephenson, R. O., Yamanaka, Y. and Rossant, J. (2010). Disorganized epithelial polarity and excess trophectoderm cell fate in preimplantation embryos lacking E-cadherin. *Development* **137**, 3383-3391.

Strumpf, D., Mao, C. A., Yamanaka, Y., Ralston, A., Chawengsaksophak, K., Beck, F. and Rossant, J. (2005). Cdx2 is required for correct cell fate specification and differentiation of trophectoderm in the mouse blastocyst. *Development* **132**, 2093-2102.

Tepass, U. (2012). The apical polarity protein network in Drosophila epithelial cells: regulation of polarity, junctions, morphogenesis, cell growth, and survival. *Annu. Rev. Cell Dev. Biol.* **28**, 655-685.

Tojkander, S., Gateva, G. and Lappalainen, P. (2012). Actin stress fibers – assembly, dynamics and biological roles. *J. Cell Sci.* **125**, 1855-1864.

Valdez Magaña, G., Rodríguez, A., Zhang, H., Webb, R. and Alberio, R. (2014). Paracrine effects of embryo-derived FGF4 and BMP4 during pig trophoblast elongation. *Dev. Biol.* **387**, 15-27.

van Eijk, M. J. T., van Rooijen, M. A., Modina, S., Scesi, L., Folkers, G., van Tol, H. T., Bevers, M. M., Fisher, S. R., Lewin, H. A., Rakacolli, D. et al. (1999). Molecular cloning, genetic mapping, and developmental expression of bovine POU5F1. *Biol. Reprod.* **60**, 1093-1103.

Watson, A. J. (1992). The cell biology of blastocyst development. *Mol. Reprod. Dev.* **33**, 492-504.

Wiley, L. M. (1988). Trophectoderm: the first epithelium to develop in the mammalian embryo. *Scanning Microsc.* **2**, 417-426.

Wu, G. and Schöler, H. R. (2011). Role of mouse maternal Cdx2: what's the debate all about? *Reprod. Biomed. Online* **22**, 516-518.

Wu, G., Gentile, L., Fuchikami, T., Sutter, J., Psathaki, K., Esteves, T. C., Arauzo-Bravo, M. J., Ortmeier, C., Verberk, G., Abe, K. et al. (2010). Initiation of trophectoderm lineage specification in mouse embryos is independent of Cdx2. *Development* **137**, 4159-4169.

Xia, P., Liu, Z. and Qin, P. (2011). Fine structures of embryonic discs of in vivo post-hatching porcine blastocysts at the pre-primitive streak stage. *Reprod. Domest. Anim.* **46**, 366-372.

Yoshioka, K., Suzuki, C., Tanaka, A., Anas, I. M. and Iwamura, S. (2002). Birth of piglets derived from porcine zygotes cultured in a chemically defined medium. *Biol. Reprod.* **66**, 112-119.

Zhi, Y., Jia, G., Gerelchimeg, B., Shi-chao, L., Yan-shuang, M. and Zhong-hua, L. (2014). Lentivirus mediated gene manipulation in trophectoderm of porcine embryos. *J. Northeast Agric. Univ.* **21**, 39-45.

Supplementary Information

Supplementary Figures:

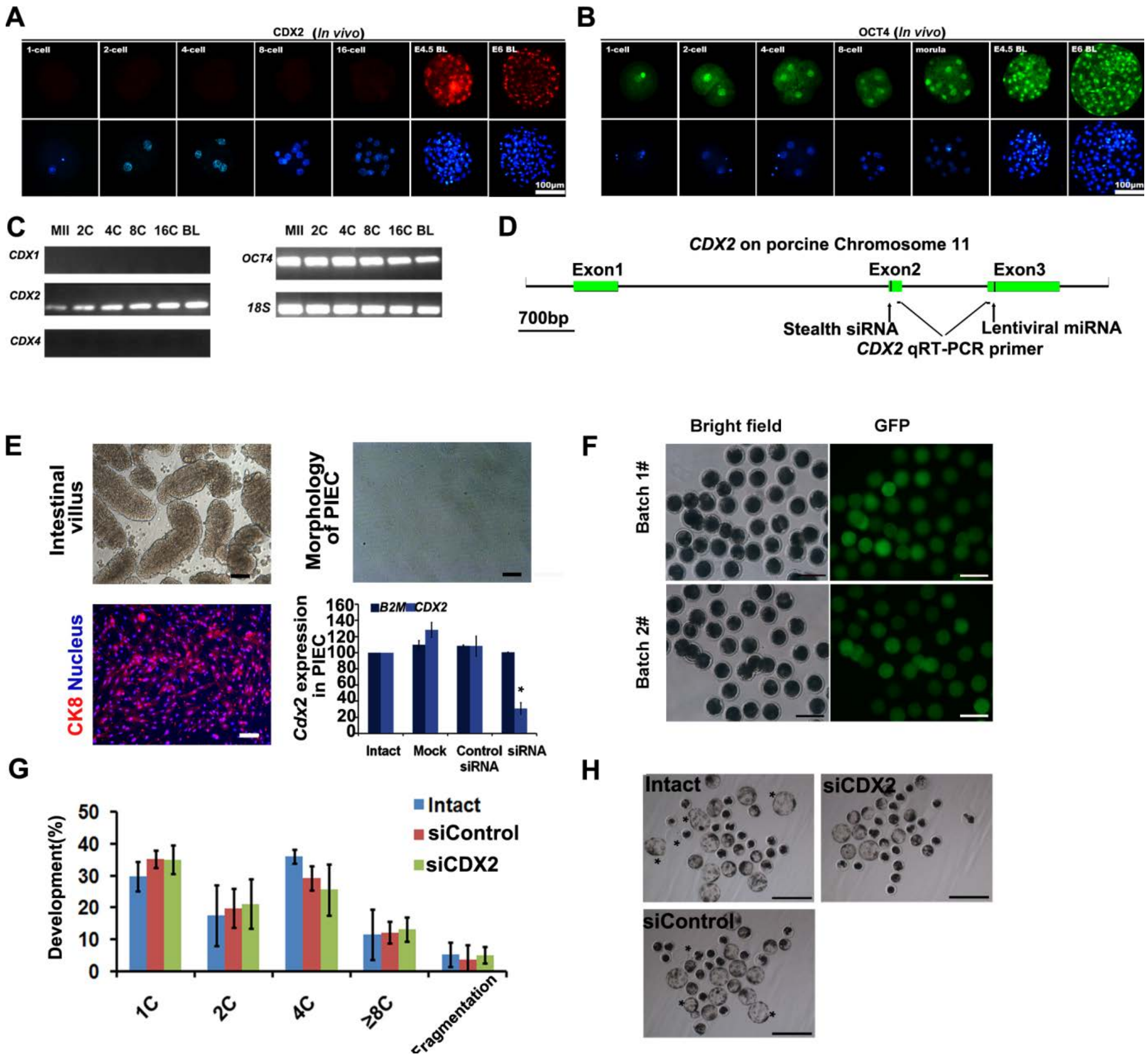

Fig. S1 The effects of *CDX2* knockdown on porcine embryonic development. (A-B) IF assays shows the *in vivo* expression pattern of (A) OCT4 (green) and (B) CDX2 (red). (C) RT-PCR proved the *CDX2* and *OCT4* mRNA expression throughout the development and the absence of *CDX1* and *CDX4* expression in porcine early stage embryos. (D) Illustration of locus targeted by CDX2 interfering tools and primers for qPCR. This study used two methods to knockdown *CDX2*: Stealth siRNA injection in zygotes and miRNA- expressing lentivirus mediated CDX2 knockdown. “Stealth siRNA” and “Lentiviral miRNA” labeled their target locus. (E) Stealth siRNA also could effectively repress CDX2 expression in porcine intestinal epithelial cells (PIEC). Bar, 100µm. (F) Injection of GFP mRNA into porcine zygotes has shown that our injection efficiency is close to 100%. Bar, 100µm. (G) The morphology of embryos at D6.5. Bar, 500µm. (H) Embryonic development at D3.

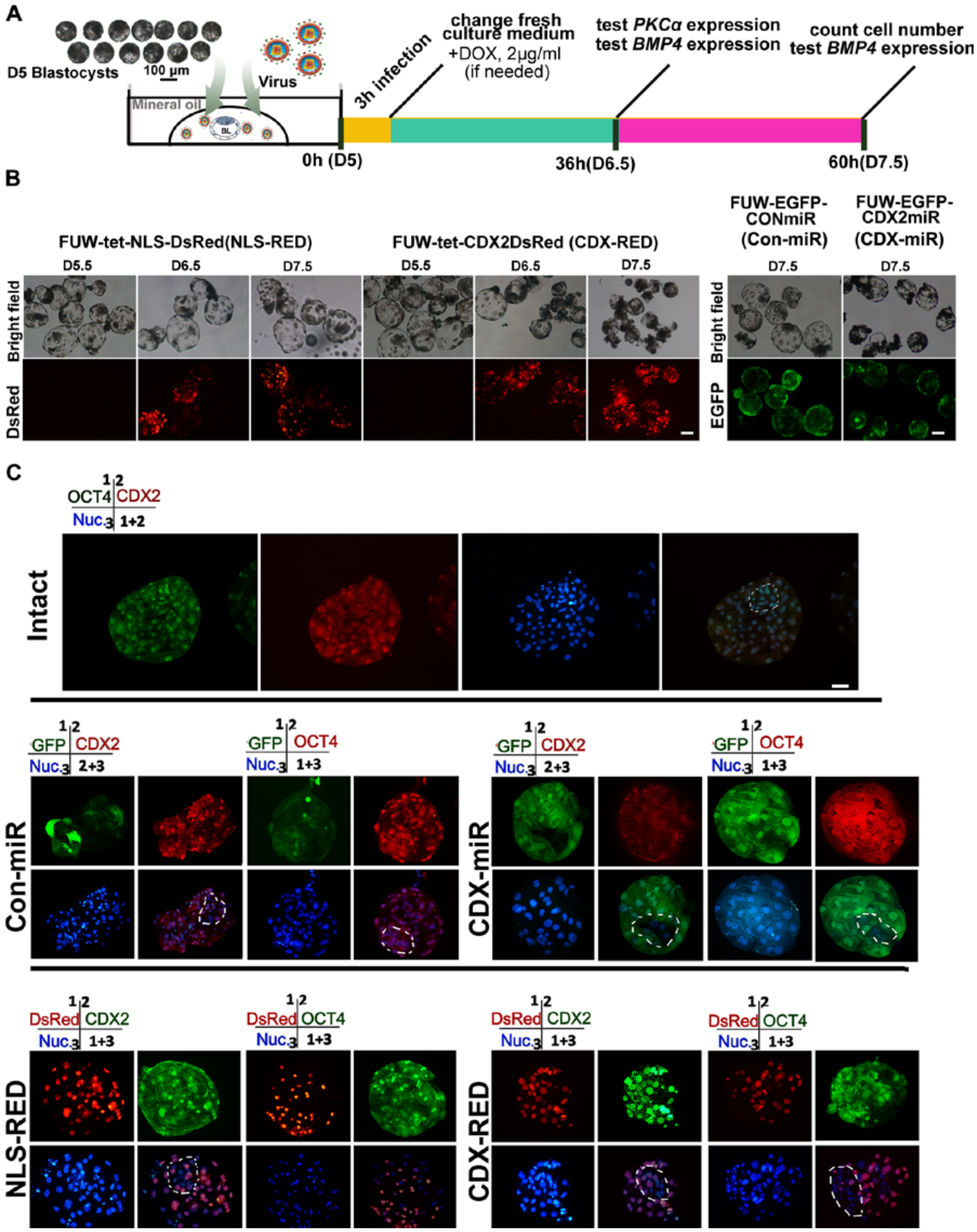

Fig. S2 Lentivirus mediated TE specific *CDX2* regulation. (A) The procedure of lentivirus infection and following experiments. (B) The status of blastocysts after lentivirus transfection. (C) IF assay shows the CDX2 and OCT4 expression after TE specific lentivirus infection. Bar, 50µm.

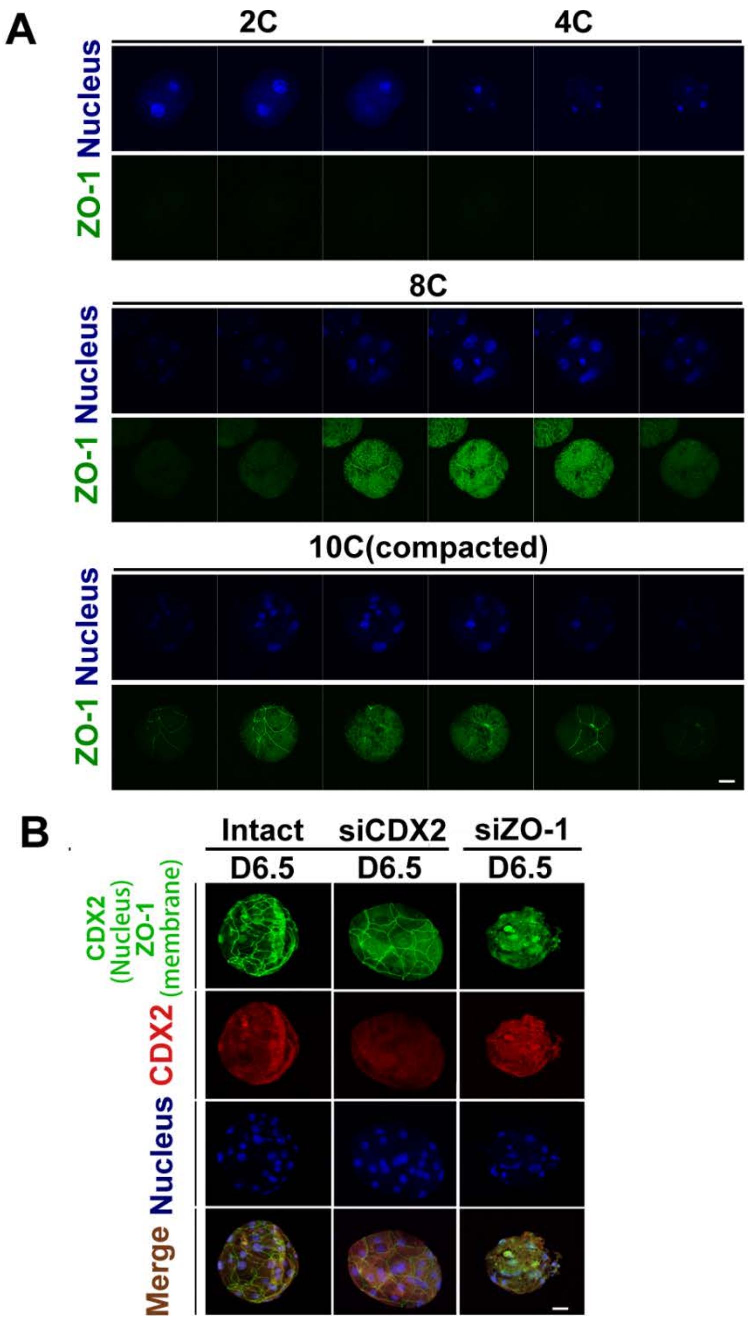

Fig. S3 CDX2 expression and the tight junction formation are independent events. (A) IF assay against ZO-1 in cleavage stage porcine embryos indicates that the formation of tight junction in porcine embryos is earlier than the CDX2 accumulation. (B) IF results show that the formation of tight junction (marked by ZO-1) and CDX2 expression are independent, because RNA interference against each of them does not affect the another one. Bar, 50μm.

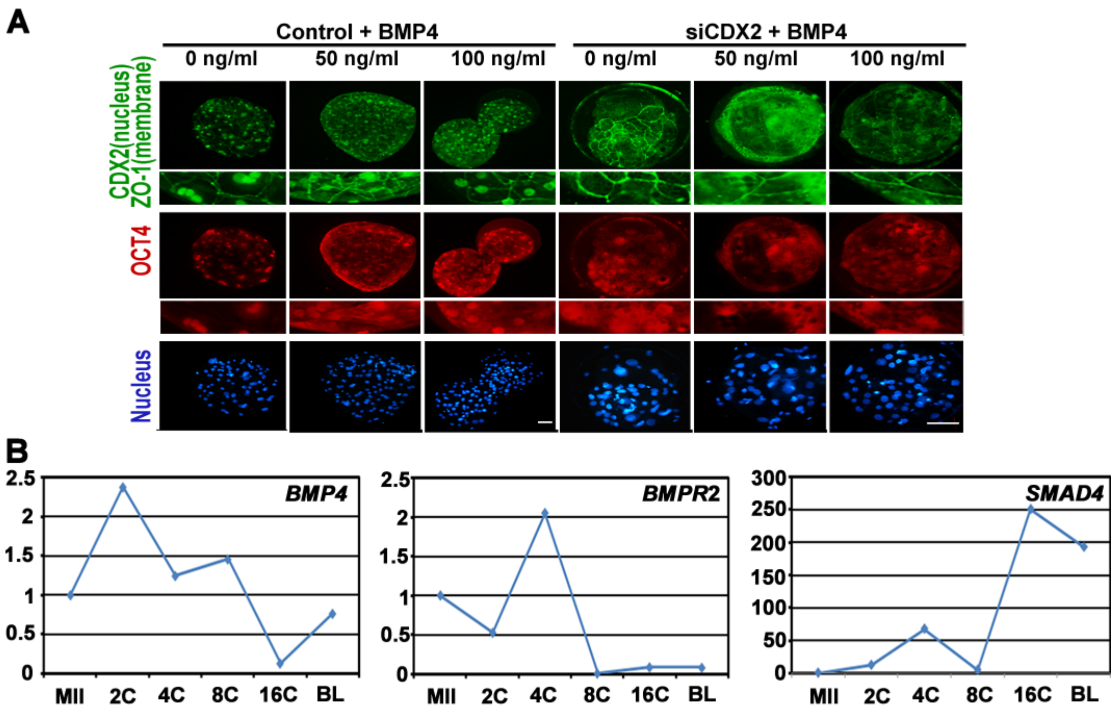

Fig. S4 BMP4 signaling is active in porcine blastocysts. (A) IF assay was used to calculate the blastocyst cell numbers after BMP4 supplement and at the same time prove CDX2 absence in siCDX2 blastocysts. Bar, 50µm. (B) The mRNA expression patterns of *BMP4*, *Smad4* and *BMPR2* throughout early porcine embryo.

Supplementary Tables：

Table S1. Primers used for qPCR

Gene	GeneBank No.(Ensemble ID)	Primer pairs
CDX2	AM778830	F：5'AGTCGCTACATCACCATTCGGAG3' R：5'GCTGCTGTTGCTGCAACTTCTTC3 '
POU5F1	NM_001113060	F： 5'GAAGCTGGACAAGGAGAAGCTGGAG3 ' R：5'ATGGTCGTTTGGCTGAACACCTTC3 '
NANOG	AY596464	F：5'CCTCCATGGATCTGCTTATTC3 ' R：5'CATCTGCTGGAGGCTGAGGT 3 '
SOX2	NM_001123197	F：5'AACCAGAAGAACAGCCCAGAC3 ' R：5'TCCGACAAAAGTTTCCACTCG3 '
GATA4	NM_214293	F：5'ATGAAGCTCCATGGTGTCCC 3 ' R：5'ACTGCTGGAGTTGCTGGAAG3 '
GATA6	NM_214328	F：5'TTGGTTATTCCCGAATTTCTCCG3 ' R：5'CATTCCTGCAAACTGGGTGATAC3 '
CDH1	NM_001163060.1	F：5'TGCTGCTCCTGCTCCTTATTCG3 ' R：5'CTGGTCCTCTTCTCCACCTCCT3 '
ZO-1	AJ318101.1	F：5'AGTGGCGTTGACACGTTCTCTG3 ' R：5'ACCACGGTGTGACCATCCTCAT3 '
PRKCA	XM_005668672.1	F：5'GGAGACAGCCTTCCAACAACCT3 ' R：5'TGTCGGCGAGCATCACCTTC3 '
ATP1B1	AJ401029.1	F：5'TGTGCCCAGCGAACTCAAAGAA3 ' R：5'CCAACCATTCGAGCCTGAACCT3 '
EOMES	XM_003132081.2	F: 5'TGGACTCAATCCTACTGCCCACTAC3 ' R：5'TTTGCCGCAGGTCACCCACTT3 '
ELF5	NM_001243711.1	F：5'TCCTCCAGAACATTCGCTCACAAG3 ' R： 5'TGATGAGAACTTTGGAGGCTTGTTC3 '
CDH3	（ENSSSCT00000026686.1）	F: 5'GTCACAGACCAGAACGACCACAAG3 ' R：5'CATCGTCCTCATCGGTGGCTGT3 '
HAND1	NM_001014428.1	F：5'CCGAGCTGCGCGAGTGCAT3 ' R：5'TTGGCCAGCACGTCCATCAGGT3 '
GCM1	XM_001927486.5	F：5'CCTTTCTCCTCACCTATACCTCTC3 ' R：

Table S2. Antibodies Used for IF and WB assays

Primary antibody			
Immunogen	Source	Dilution	Description
a peptide mapping near the N-terminus of Oct-3/4 of human origin	sc-8628 Santa Cruz	IF:1:50	OCT4, Goat polyclonal IgG
human CDX2 recombinant protein	ab-88129 Abcam	IF:1:50 WB:1:500	CDX2, Rabbit monoclonal IgG
Human E-Caherin	ab-1416 Abcam	IF:1:50	E-CADHERIN, Mouse monoclonal IgG1
Human ZO-1	339188 Invitrogen	IF:1:500	Mouse monoclonal antibody conjugated to Alexa Fluor 488
A synthetic peptide corresponding to internal region of human NANOG	PAB6837 Abnova	IF:1:50	NANOG, Goat polyclonal
a peptide mapping near the C-terminus of Sox-2 of human origin	sc-17320 Santa Cruz	IF:1:100	SOX2, Goat polyclonal IgG
peptide region of the Human ZFP42 protein sequence according to NP_777560	SAB210276 9 Sigma	IF:1:100	ZFP42(REX1), Rabbit polyclonal
Human Cytokeratin-18	BM0032 Boster	IF:1:100	CK8, Mouse monoclonal IgG
a peptide from the p17 fragment corresponding to the cleaved region of caspase-3 human caspase-3	G7481 Promega	IF:1:500	Active- CASPASE3, Rabbit polyclonal
synthesized peptide derived from human Catenin-β	SAB450054 3 Sigma	IF:1:100	endogenous levels of total CATNB (Catenin-β), Rabbit polyclonal IgG
the C-terminus of PKC ζ of rat origin	sc-216 Santa Cruz	IF:1:50	PKCζ, Rabbit polyclonal IgG
residues surrounding Thr567 of human ezrin,	3149P CST	IF:1:500 WB:1:100 0	Phospho-Ezrin (Thr567), Rabbit monoclonal IgG
amino acids 311-586 mapping at the C-terminus of human Ezrin	sc-20773 Santa Cruz	IF:1:500 WB:1:100 0	Total Ezrin, Rabbit polyclonal IgG
the C-terminus of PKCα of human origin	sc-208 Santa Cruz	IF:1:500 WB:1:100	PKCα, Rabbit polyclonal IgG

Secondary antibody

Name	Source
Alexa Fluor 546 Donkey Anti-Rabbit IgG	Molecular Probe A10040
Alexa Fluor 546 Donkey Anti-Mouse IgG	Molecular Probe A10036
Alexa Fluor 546 Donkey Anti-Goat IgG (H+L)	Molecular Probe A11056
Alexa Fluor 488 Donkey Anti-Goat IgG (H+L)	Molecular Probe A11055
Alexa Fluor 488 Doncky Anti-Rabbit IgG (H+L)	Molecular Probe A21206
Alexa Fluor 488 Donkey Anti-Mouse IgG (H+L)	Molecular Probe A21202
Anti-Rabbit IgG (whole molecule) –Peroxidase antibody produced in goat	Sigma A9169
Anti-Mouse IgG (whole molecule) –Peroxidase antibody produced in rabbit	Sigma A9044

Note Commercial antibodies have been tested and found to not work in pig including :

OCT4: sc-8629 Santa Cruz; O8389 Sigma
CDX2: AB4123 Millipore; 3977S Cell Signaling
NANOG: sc-33760 Santa Cruz; ab21624 Abcam
SOX2: ab97959 Abcam
ZFP42: ab50828 Abcam